RSC Advances

ROYAL SOCIETY OF CHEMISTRY

www.rsc.org/advances

Self-assembly of phosphorescent quantum dots / Boronic-Acid-Substituted Viologens nanohybrids based on photoinduced electron transfer for glucose detection in aqueous solution

Yanming Miao Maoqing Yang Guiqin Yan*

Shanxi Normal University, Linfen 041004, PR China

* Corresponding author. Tel.: (86) 357-2051249; Fax.: (86) 357-2051243.
E-mail: gqyan2013@163.com.

Abstract: We synthesized boronic-acid-substituted viologens (BBV) and designed a glucose sensor based on room-temperature phosphorescence (RTP) quantum dots (QDs) and BBV. This sensor utilizes 3-mercaptopropionic acid (MPA)-capped Mn-doped ZnS QDs as an RTP indicator as well as BBV as an RTP quencher and a glucose detection receptor. At physiological pH 7.4, the negatively-charged MPA-capped Mn-doped ZnS QDs and the positively-charged BBV interact via electrostatic attraction to form composites, which quench the RTP of MPA-capped Mn-doped ZnS QDs via Photoinduced Electron Transfer (PIET). After addition of glucose into this two-component system, it binds with boric acid to form a tetrahedral anionic borate, which effectively neutralizes the positive charge of BBV and deprives BBV from the QDs, thereby restoring the RTP. On this basis, this new sensor is built for glucose detection. This sensor has a detection limit of 0.09 mM and two linear ranges from 0 to 4 mM and from 4 to 16 mM, respectively. This sensor is featured with enzyme independence, simple design and easy operation.

Keywords: Glucose; Phosphorescence; Sensor; Boronic-acid-substituted viologens

Glucose plays an extremely important role in organisms, since it is involved in many biological and pathological processes. Glucose transport is the main energy source for organism metabolism, but its breakdown is correlated with the occurrence of renal glycosuria, signal transduction, cell adhesion, cystic fibrosis, diabetes and some cancers in humans.[1-6] Thus, real-time accurate glucose detection is very important.

At present, the main challenge in diabetes control is how to accurately trace the glucose concentration. Glucose oxidase (GOD) is employed in many sensors for optical and electrochemical glucose determination based on the enzyme-catalyzed oxidation mechanism.[7-12] However, since these glucose sensors are mostly based on enzymes (e.g. GOD and glucose dehydrogenase), they are faced with inevitable defects: frequent and extremely inconvenient blood sampling, detection discontinuity, harsh test conditions, instability, and limitation to only a few types of glucoses. Nevertheless, these defects in glucose detection can be overcome by using phenylboronic compounds as a recognition receptor. Boric acid and its derivatives, which can bind with glycol via reversible and efficient covalent bonds to form circular borate, can all be used as a molecular probe of biological sensors to identify glucose compounds.[13, 14] Compared with conventional glucose sensors, the boric-acid- based sensors are more promising with lower cost, higher stability, and reversibility in regeneration. However, the optimal pH for glucose identification is generally ≥ the pKa of boric acid and most of its synthetic derivatives (pKa 8-9), which becomes the bottleneck in boric-acid-based glucose detection.

Recently, the detection based on room-temperature phosphorescence (RTP) quantum dots (QDs) has attracted much attention and is widely applied into sensors, especially biomolecular sensors.[15-32] Owing to the longer lifetime of phosphorescence than fluorescence, RTP-QDs-based detection shows high reliability and stability without the interference from autofluorescence or scattered light.[15, 19] Since phosphorescence is less common than fluorescence, the detection selectivity of RTP QDs can be further enhanced.[16] Moreover, the existing biosensors based on RTP QDs do not need any complicated sample pretreatment.[17, 19, 24]

In this study, boronic-acid-substituted viologen (BBV) was synthesized from 2-(bromomethyl)phenylboronic acid and 4,4'-bipyridyl. Then a glucose detection sensor based on RTP QDs and BBV was designed. This sensor is able to detect glucose at physiological pH 7.4 by using boric acid derivatives. It utilizes 3-mercaptopropionic acid (MPA)-capped Mn-doped ZnS QDs as an RTP indicator, BBV as an RTP quencher, and a glucose receptor (Fig. 1). At the physiological pH 7.4, the negatively-charged MPA-capped Mn-doped ZnS (rich in -COOH) QDs interact via electrostatic attraction with the positively-charged BBV to form composites. Thereby, the electron transfer from the MPA-capped Mn-doped ZnS QDs to the strong electron-rich BBV will quench the RTP of the QDs. After addition of glucose into this two-component system, it will bind with boric acid to form a tetrahedral anionic borate, which effectively neutralizes the positive charge of BBV and largely quenches the MPA-capped Mn-doped ZnS QDs, thereby restoring the RTP.

2. Experimental

2.1. Materials and Chemicals

MPA (J&K Scientific, Beijing, China), $Zn(Ac)_2 \cdot 2H_2O$, $Mn(Ac)_2 \cdot 4H_2O$, and $Na_2S \cdot 9H_2O$ (all Tianjing Kermel Chemical Reagent Co., China) were used to prepare Mn-doped ZnS QDs. Ultrapure water (18.2 MΩ cm) was obtained from a Water Pro water purification system (Labconco Corporation, Kansas City, MO, USA). Other materials included 2-bromomethyl-phenylboronic acid (Sigma Chemical Co., St. Louis, USA), 4,4'-dipyridyl (J&K Scientific, Beijing, China), and glucose (Tianjing Kermel Chemical Reagent Co., China).

2.2. Apparatuses

The morphology and microstructure of the QDs were characterized by a JEM-2100 transmission electron microscope (TEM, JEOL Ltd., Japan). Phosphorescence was measured by a Cary Eclipse fluorescence spectrophotometer (Varian American Pty Ltd., USA), equipped with a plotter unit and a quartz cell (1 cm × 1 cm) in the phosphorescence mode. pH was measured with a pH meter (Jinpeng Analytical Instruments Co. Ltd, China). ^{1}H nuclear magnetic resonance (^{1}H NMR) was measured on a Bruker-600M HZ instrument (Bruker Corporation, Germany) with Methanol-D4 as the solvent. Also a Varian640 Fourier transform infrared (FT-IR) spectrometer (Varian American Pty Ltd., USA) was used. The p*K*a was measured with a pION Gemini Profiler (Pion Co. Ltd, USA).

2.3. Synthesis of Mn-Doped ZnS QDs

Mn-Doped ZnS QDs were synthesized in aqueous solutions as per a published method[19, 33] with minor modification. The specific steps are showed below. First, 5

mL of 0.1 M $Zn(Ac)_2$, 2 mL of 0.01 M $Mn(Ac)_2$, and 50 mL of 0.04 M MPA were added to a three-neck flask. The mixture was adjusted to pH 11 with 1 M NaOH. After 30 min of argon ventilation at room temperature, the mixture was injected with 5 mL of 0.1 M Na_2S via injection. After stirring for 20 min, the solution was aged at 50 ℃ and open air for 2 h. The resulting QDs were purified successively by precipitation with ethanol, centrifugation, washing with ethanol, and vacuum drying.

2.4. Synthesis of BBV

The synthesis process of BBV from 2-(bromomethyl) phenylboronic acid and 4,4'-bipyridyl is showed in Fig. S1. The specific steps are showed below.[34, 35] First, 4.05 mM 2-(bromomethyl)phenylboronic acid was dissolved into 15 mL of N,N-dimethylfomamide (DMF), which were poured into a 50 mL three-necked bottle equipped with a magnetic stirrer; then the solution was added with 1.6 mM 4,4'-bipyridyl and mixed under argon protection and 70 □ for 48 h. Solids were formed after cooling and filtration, and then washed with DMF, acetone and ether successively. The final product BBV was prepared after vacuum-drying. The product was characterized by FT-IR and ^1H NMR.

2.5. Assay conditions and RTP measurement

To study the BBV effect of the MPA-capped Mn-doped ZnS QDs on the RTP intensity, we prepared a 4.0×10^{-5} M mother liquor from BBV. Then different volumes of the mother liquor were added into a phosphate-buffered saline solution (PBS, pH 7.4, 10 mM) to form different BBV solutions. MPA-capped Mn-doped ZnS QDs were dissolved in water to form a 2.0 mg mL^{-1} solution, which (100 μL) was

then added to each of the above BBV solutions. After 5 min, the RTP was measured. For glucose detection, the salmon sperm glucose was made into a 100 mM mother liquor. The assay solutions containing MPA-capped Mn-doped ZnS QDs (100 μL), BBV (200 μL), and different concentrations of glucose (0 - 40 mM) were prepared in 5 ml of PBS (10 mM, pH 7.4). Reactions proceeded for 5 min before spectrophotometry.

3. Results and discussion

3.1. Characterization of the MPA-capped Mn-doped ZnS QDs

The size of the MPA-capped Mn-doped ZnS QDs was tested by TEM to be ~3.5 nm (Fig. S2a). The maximum excitation peak occurred at 295 nm and a narrow emission band was centered at 590 nm: hv_1 is the fluorescence occurring from the surface defect of ZnS QDs; hv_2 is the phosphorescence attributed to the transition of Mn^{2+} from the triplet state ($^4T_1$) to the ground state ($^6A_1$) (Fig. S2b). As reported, Mn-doped ZnS QDs exhibit an orange phosphorescence emission (about 590 nm),[36] which is attributed to the energy transfer from the band gap of ZnS to the dopant Mn^{2+} and the subsequent $^4T_1$-to-$^6A_1$ transition of the Mn^{2+} incorporated into the ZnS lattice.[37]

3.2. Characterization of the BBV

The infrared spectra of BBV measured with KBr tablet compression (Fig. S3) show peaks at 3408, 3019, 2962, 1639, 1597/1505, 1448 and 1324 cm^{-1}, which are attributed to the stretching vibrations of O-H, benzonic C-H, -CH_2 (asymmetric and symmetric), C=N, benzene ring skeleton, C-N, and B-O (asymmetric), respectively.

These results are basically consistent with two previous reports.[34, 35]

The structure of BBV was further characterized via ^{1}H NMR with Methanol-D4 as a solvent. The results are δ 9.01 (d, J = 7.2 Hz, 4H), 8.42 (d, J = 7.2 Hz, 4H), 7.75 (d, J = 6.6 Hz, 2H), 7.57 (t, J = 6.0 Hz, 2H), 7.52(m, 4H), and 6.04 (s, 4H) (Fig. S4).

The p*K*a of BBV was further measured with a acid-base titration, $pK_a^{25\ ^{\circ}C}$=8.08.

3.3. Interaction of MPA-capped Mn-doped ZnS QDs with BBV

With the increase of BBV concentration, the RTP intensity of the QDs is gradually quenched at 590 nm (Fig. 2a) and basically unchanged after the addition of 1.6 μM BBV (Fig. 2b). The RTP intensity of the nanohybrids was basically stable after 5 min (Fig. S5a).

At pH 7.4, the MPA-capped Mn-doped ZnS QDs are negatively charged owing to the presence of -COOH. However, since the surface of BBV is positively charged, BBV and QDs electrostatically interact to form a Mn-doped ZnS QDs/BBV complex. Such electrostatic interaction can be validated by the variation of zeta-potential and the quenching intensity under varying ionic strength. As showed in Fig. 2c, the zeta potential of pure QDs solution is -29.6 mV. After the addition of BBV, it interacts electrostatically with QDs to form a complex, which reduces the negative charge around the QDs and thus changes the zeta potential to -18.3 mV. After addition of glucose, it interacts with boric acid to form borate and thus neutralizes the positive charge of BBV, thereby depriving BBV from the surface of QDs and restoring the zeta potential to -28.7 mV.

Figure 2d shows the response curve of QDs quenching at varying ionic strength. Clearly, the QDs quenching rate is reduced with the increase of ionic strength. With the increase of ion concentration, more cations are adsorbed onto the surface of the negatively-charged QDs to neutralize the surface negative charge, thereby inhibiting the QDs-BBV electrostatic interaction and reducing the QDs quenching rate.

3.4. Mechanism of BBV in quenching the RTP of Mn-doped ZnS QDs

The quenching of QD with methyl viologen (MV^{2+}) has already been reported.[38-44] This process occurs through an excited-state electron transfer from the QD to the viologen, resulting in the reduced viologen to $MV^{\cdot+}$. Viologen is extremely efficient in statically quenching the fluorescence of many organic dyes by forming a complex with fluorophore.[45, 46] We reason that the RTP of Mn-doped ZnS QDs bears surface polar groups, or that the complex formation with BBV quenchers might similarly quench the carboxy groups. Thus, BBV might quench the RTP of Mn-doped ZnS QDs through the Photoinduced Electron Transfer (PIET) (Fig. 3).

3.5. Detection of Glucose using Mn-doped ZnS QDs/BBV complex

The RTP intensity of the Mn-doped ZnS QDs/BBV was gradually and regularly enhanced with the increase of glucose content (Fig. 4a). Figure 4b illustrates the recovering process of QDs after the addition of glucose. The RTP intensity of the glucose sensor was basically stable after 5 min (Fig. S5b).

In comparison, with the absence of BBV, the increase of glucose content between 0 and 20 mM does not severely change the RTP intensity of separate Mn-doped ZnS QDs (Fig. 4c).

3.6. Working mechanism between glucose and BBV

As reported, the phenylboronic acid compounds and saccharides in alkaline solutions can bind reversibly to form five- or six-member ring esters.[47] In the present study, therefore, the reaction between BBV phenylboronic compounds and saccharides in alkaline solutions can be divided into two steps (Fig. 5). (1) Boric acid is hydroxylated in the alkaline solution, and -OH attacks the electron-free orbit in B to form a tetrahedral anionic borate. At this moment, the configurations of both B and compounds are changed dramatically. (2) The boric acid anions formed in step (1) bind with glycol to form five- or six-member ring esters.

The tetrahedral anionic borate formed from glucose and BBV can effectively neutralize the positive charge of BBV, thus largely weakening the electrostatic bonding ability between the MPA-capped Mn-doped ZnS QDs and BBV. As a result, BBV falls off from the Mn-doped ZnS QDs to recover their RTP.

3.7. Characterization of Mn-doped ZnS QDs as RTP probes

Based on these results, a quantitative glucose detection sensor with the use of Mn-doped ZnS QDs RTP was designed. RTP was quenched by the complex formed between BBV and Mn-doped ZnS QDs, but was gradually recovered by adding different contents of glucose into the complex. Under pH 7.4, the RTP recovery rate (RTP/RTP_0) and the glucose concentration are linearly related within modest ranges (Fig. 6).

The linear ranges of glucose concentration are 0-4 mM and 4-16 mM, with the linear equations $RTP/RTP_0 = 0.338\ C_{glucose} + 1.028$ ($R = 0.998$) and $RTP/RTP_0 =$

219 0.120 $C_{glucose}$ + 1.877 (R = 0.993), respectively. This new sensor has a detection limit
220 (3σ) of 0.09 mM. For systems with 0.4 mM glucose RTP, the relative standard
221 deviation of 11 continuous parallel detections is 2.7%.

222 This novel sensor outperforms other glucose detection sensors in many aspects.
223 First, no enzyme is required. Second, compared with some fluorescence detection
224 methods,[48-51] this boric-acid- based sensor is featured with lower cost, higher stability,
225 reversibility in regeneration, and in particular, higher ability in glucose detection at
226 physiological pH 7.4.

227 Since RTP compared with fluorescence is a rarer phenomenon and thus is more
228 selective during detection. Moreover, RTP has a longer life and can effectively avoid
229 the interference from background fluorescence or scattering light (e.g. from biofluids).
230 RTP detection also does not require any complex pretreatment, such as addition of
231 deoxidant or revulsive. Thus, the RTP method compared with the fluorescence
232 method in Ref. 46 is simpler, more efficient and more stable in real applications.
233 Moreover, since RTP can efficiently avoid the interference of background
234 fluorescence and scattering in biofluids, our method has wide application prospects
235 for glucose detection in biofluids.

236 **4. Conclusions**

237 A sensitive sensor for quantitative glucose detection was designed. BBV was
238 adsorbed via electrostatic attraction onto the surface of MPA-capped Mn-doped ZnS
239 QDs, quenching the phosphorescence of the QDs via PIET and rendering the restore
240 of RTP. With the addition of glucose, BBV intercalated with glucose and was

competitively induced to fall off from the surface of the QDs, thus recovering the RTP of the QDs. Based on this, the new sensor was built. It has a detection limit of 0.009 mM and two linear ranges from 0 to 4 mM and from 4 to 16 mM respectively. This sensor has simple operations and enzyme independence.

Acknowledgment

This work was supported by the funds of Shanxi Normal University (ZR1501) and School of Life Science (SUYKZ-41).

References

1 T.D. James, K.R.A.S. Sandanayake, S. Shinkai, *Angew. Chem. Int. Edit.*, 1996, 35, 1910-1922.

2 E.I. Buzás, E.I. Buzás, B. György, E.I. Buzás, B. György, M. Pásztói, I. Jelinek, A. Falus, H.J. Gabius, *Autoimmunity*, 2006, 39, 691-704.

3 A. Heller, B. Feldman, *Chem. Rev.*, 2008, 108, 2482-2505.

4 K.S. Lau, J.W. Dennis, *Glycobiology*, 2008, 18, 750-760.

5 H.E. Murrey, L.C. Hsieh-Wilson, *Chem. Rev.*, 2008, 108, 1708-1731.

6 K. Jayakanthan, S. Mohan, B.M. Pinto, *J. Am. Chem. Soc.*, 2009, 131, 5621-5626 .

7 P.W. Barone, R.S. Parker, M.S. Strano, *Anal. Chem.*, 2005, 77, 7556-7562.

8 J.C. Pickup, F. Hussain, N.D. Evans, O.J. Rolinski, D.J.S. Birch, *Biosensors Bioelectron.*, 2005, 20, 2555-2565.

9 V. Vamvakaki, K. Tsagaraki, N. Chaniotakis, Anal. Chem., 2006, 78, 5538-5542.

10 T. Zhang, E.V. Anslyn, *Org. Lett.*, 2007, 9, 1627-1629.

11 Y.C. Shiang, C.C. Huang, H.T. Chang, *Chem. Commun.*, 2009, 3437-3439.

12 T.W. Tsai, G. Heckert, L.F. Neves, Y. Tan, D.Y. Kao, R.G. Harrison, D.E. Resasco, D.W. Schmidtke, *Anal. Chem.*, 2009, 81, 7917-7925.

13 R. Nishiyabu, Y. Kubo, T.D. James, J.S. Fossey, *Chem. Commun.*, 2011, 47, 1106-1123.

14 X. Wu, Z. Li, X.X. Chen, J.S. Fossey, T.D. James, Y.B. Jiang, *Chem. Soc. Rev.*, 2013, 42, 8032-8048.

15 J.M. Costa-Fernández, R. Pereiro, A. Sanz-Medel, *TrAC Trends in Analytical*

Chemistry, 2006, 25, 207-218.

16 J.M. Traviesa-Alvarez, I. Sánchez-Barragán, J.M. Costa-Fernández, R. Pereiro, A. Sanz-Medel, *Analyst*, 2007, 132, 218-223.

17 Y. He, H.F. Wang, X.P. Yan, *Anal. Chem.*, 2008, 80, 3832-3837.

18 Y. He, H.F. Wang, X.P. Yan, *Chem-Eur. J.*, 2009, 15, 5436-5440.

19 P. Wu, Y. He, H.F. Wang, X.P. Yan, *Anal. Chem.*, 2010, 82, 1427-1433.

20 W.S. Zou, D. Sheng, X. Ge, J.Q. Qiao, H.Z. Lian, *Anal. Chem.*, 2010, 83, 30-37.

21 P. Wu, L.N. Miao, H.F. Wang, X.G. Shao, X.P. Yan, *Angew. Chem. Int. Ed. Engl.*, 2011, 50, 8118-8121.

22 C.X. Yang, X.P. Yan, *Anal. Chem.*, 2011, 83, 7144-7150.

23 H.B. Ren, X.P. Yan, *Talanta*, 2012, 97, 16-22.

24 E. Sotelo-Gonzalez, M.T. Fernandez-Argüelles, J.M. Costa-Fernandez, A. Sanz-Medel, *Anal. Chim. Acta*, 2012, 712, 120-126.

25 H.F. Wang, Y.Y. Wu, X.P. Yan, *Anal. Chem.*, 2013, 85, 1920-1925.

26 P. Wu, X.P. Yan, *Chem. Soc. Rev.*, 2013, 42, 5489-5521.

27 Y. Miao, Z. Zhang, Y. Gong, G. Yan, *Biosens. Bioelectron.*, 2014, 59, 300-306.

28 Y. Miao, Z. Zhang, Y. Gong, Q. Zhang, G. Yan, *Biosens. Bioelectron.*, 2014, 52, 271-276.

29 P. Wu, T. Zhao, J. Zhang, L. Wu, X. Hou, *Anal. Chem.*, 2014, 86, 10078-10083.

30 P. Wu, J. Zhang, S. Wang, A. Zhu, X. Hou, *Chemistry*, 2014, 20, 952-956.

31 P. Wu, L.N. Miao, H.F. Wang, X.G. Shao, X.P. Yan, *Angew. Chem. Int. Ed. Engl.*, 2011, 50, 8118-8121.

32 P. Wu, T. Zhao, Y. Tian, L. Wu, X. Hou, *Chemistry*, 2013, 19, 7473-7479.

33 J. Zhuang, X. Zhang, G. Wang, D. Li, W. Yang, T. Li, *J. Mater. Chem.*, 2003,13, 1853-1857.

34 L. Feng, F. Liang, Y. Wang, M. Xu, X. Wang, *Org. Biomol. Chem.*, 2011, 9, 2938-2942.

35 Y.H. Li, L. Zhang, J. Huang, R.P. Liang, J.D. Qiu, *Chem. Commun.*, 2013, 49, 5180-5182.

36 R. Thakar, Y. Chen, P.T. Snee, *Nano. Lett.*, 2007, 7, 3429-3432.

37 J.H. Chung, C.S. Ah, D.J. Jang, *J. Phys. Chem. B*, 2001, 105, 4128-4132.

38 Y. He, X. Yan, *Science China Chemistry*, 2011, 54, 1254-1259.

39 S. Logunov, T. Green, S. Marguet, M.A. El-Sayed. *J. Phys. Chem. A*, 1998, 102, 5652-5658.

40 Y. Nosaka, H. Miyama, M. Terauchi, H. Miyama. *J. Phys. Chem*., 1988, 92, 255-256.

41 M.D. Peterson, S.C. Jensen, D.J. Weinberg, E.A. Weiss. *ACS Nano*. 2014, 8, 2826-2837.

42 C. Wang, G. Cui, X. Luo, Y. Xu, H. Li, S. Dai. *J. Am. Chem. Soc*., 2011, 133, 11916–11919

43 L. Dworak, V.V. Matylitsky, V.V. Breus, M. Braun, T. Basche, J. Wachtveitl. *J. Phys. Chem. C*, 2011, 115, 3949–3955.

44 V.V. Matylitsky, L. Dworak, V.V. Breus, T. Baschéx, J. Wachtveitl.*J. Am. Chem. Soc*., 2009, 131, 2424-2425.

45 D.B. Cordes, S. Gamsey, Z. Sharrett, A. Miller, P. Thoniyot, R.A. Wessling, B. Singaram, *Langmuir*, 2005, 21, 6540-6547.

46 D.B. Cordes, S. Gamsey, B. Singaram, Angew. Chem. *Int. Ed. Engl.*, 2006, 45, 3829-3832.

47 P. John, J.O.E. Lorand, Polyol Complexes and Structure ofthe Benzeneboronate Ion., *The Journal of Organic Chemistry*, 1959, 24, 769-774.

48 X. Li, Y. Zhou, Z. Zheng, X. Yue, Z. Dai, S. Liu, Z. Tang, *Langmuir*, 2009, 25, 6580-6586.

49 J. Yuan, W. Guo, E. Wang, *Biosens. Bioelectron.*, 2008, 23, 1567-1571.

50 J. Yuan, W. Guo, J. Yin, E. Wang, *Talanta*, 2009, 77, 1858-1863.

51 M. Hu, J. Tian, H.T. Lu, L.X. Weng, L.H. Wang, *Talanta*, 2010, 82, 997-1002.

FIGURE

Fig. 1. Mechanism for glucose detection with RTP QDs.

Fig. 2 (a) BBV-concentration-dependent RTP emission of 40 mg L^{-1} MPA-capped Mn-doped ZnS QDs; (b) The change of the RTP intensity with the increase of BBV concentration; (c) The zeta-potential histogram of QDs, BBV/QDs and BBV/GQDs/glucose; (d) The effect of ionic strength on the QDs quenching degree caused by BBV.

Fig. 3. Illustrating the quenching process of QDs after the addition of BBV.

Fig. 4. (a) Glucose-concentration-dependent RTP emission of the MPA-capped Mn-doped ZnS QDs/BBV; (b) The recovering process of QDs after the addition of glucose**;** (c) Glucose-concentration-dependent RTP emission of the MPA-capped Mn-doped ZnS QDs without BBV.

Fig. 5. Mechanism in the interaction between BBV and glucose.

Fig. 6. Plots of RTP/RTP_0 as a function of glucose concentration show two linear ranges. Buffer, 10 mM PBS (pH 7.4); MPA-capped Mn-doped ZnS QDs, 40 mg L^{-1}; BBV, 1.6 μM.

373

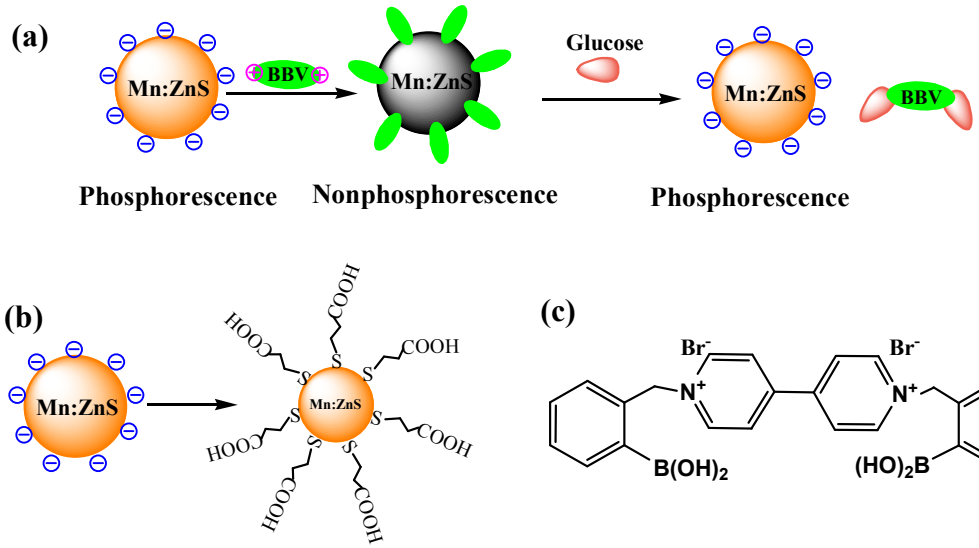

374

375 **Fig. 1.** Mechanism for glucose detection with RTP QDs.

376

377

378

379

380

381

382

383

384

385

386

387

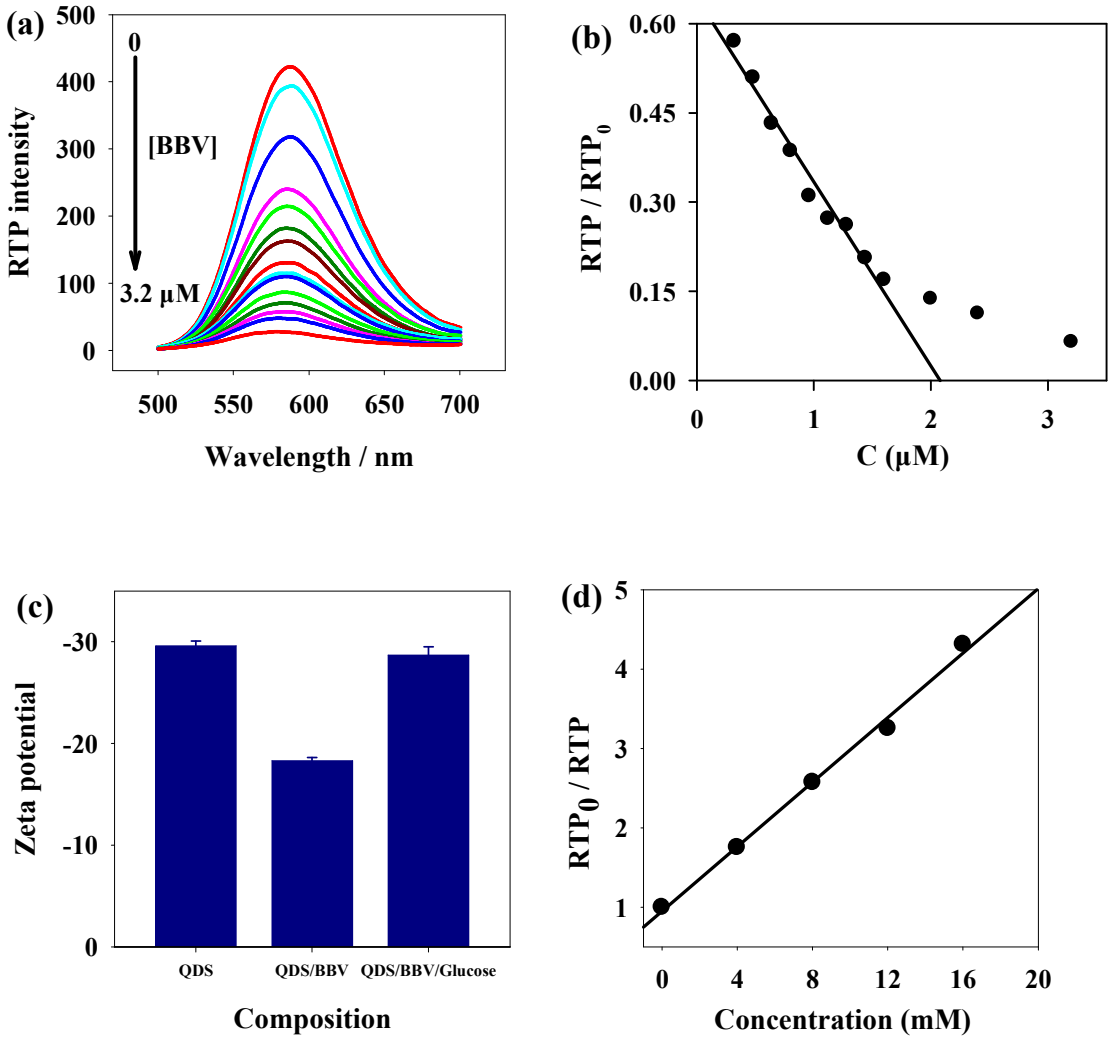

Fig. 2 (a) BBV-concentration-dependent RTP emission of 40 mg L^{-1} MPA-capped Mn-doped ZnS QDs; (b) The change of the RTP intensity with the increase of BBV concentration; (c) The zeta-potential histogram of QDs, BBV/QDs and BBV/GQDs/glucose; (d) The effect of ionic strength on the QDs quenching degree caused by BBV.

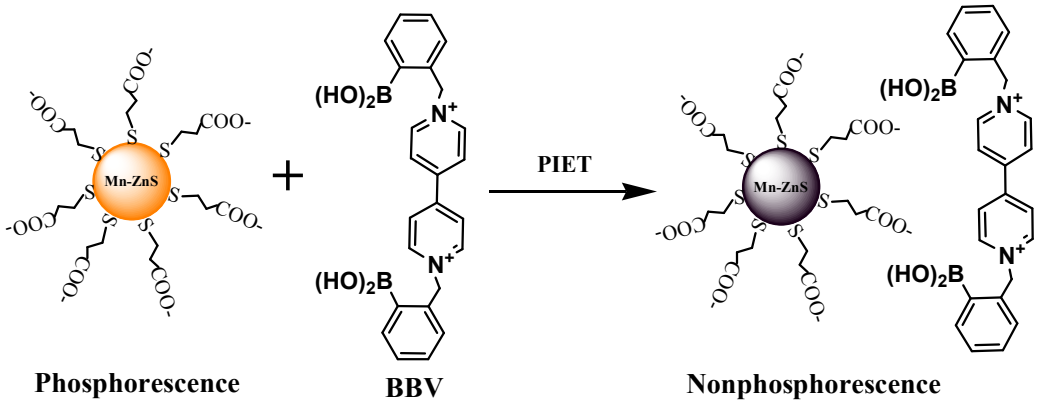

Fig. 3. Illustrating the quenching process of QDs after the addition of BBV.

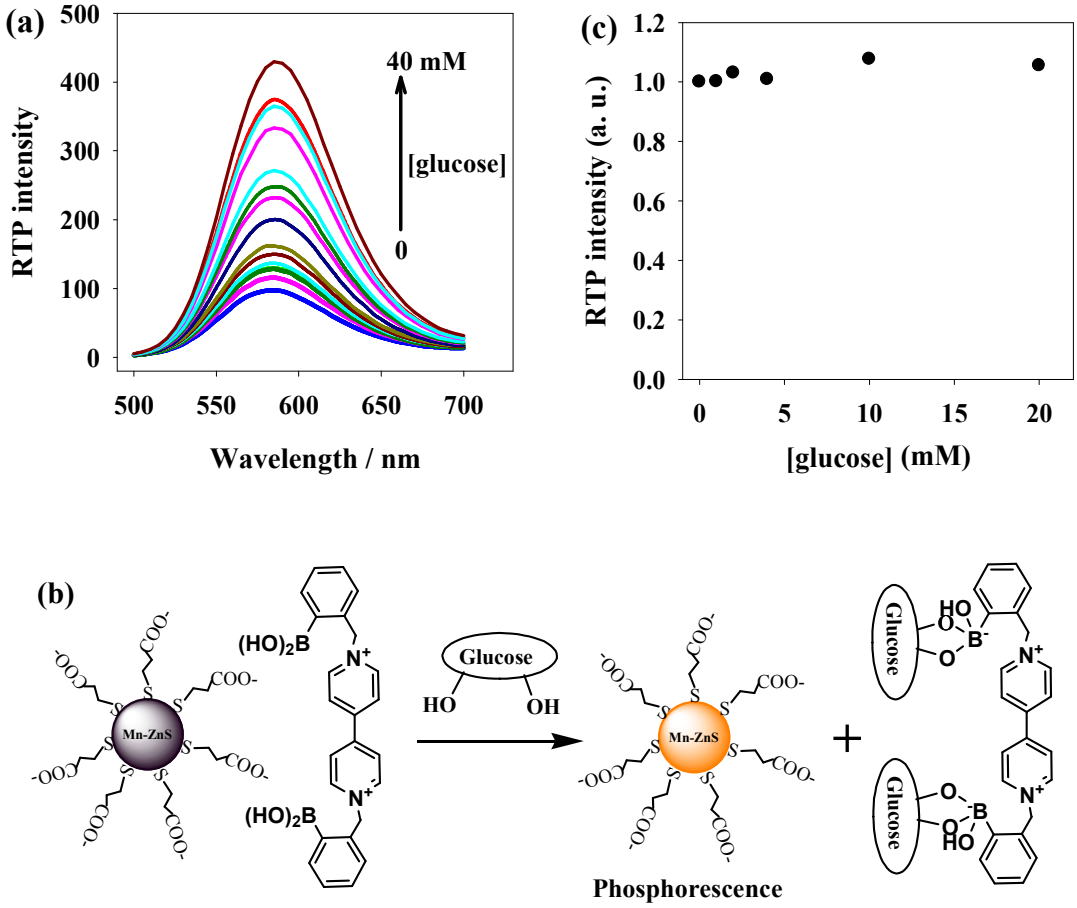

Fig. 4. (a) Glucose-concentration-dependent RTP emission of the MPA-capped Mn-doped ZnS QDs/BBV; (b) The recovering process of QDs after the addition of glucose**;** (c) Glucose-concentration-dependent RTP emission of the MPA-capped Mn-doped ZnS QDs without BBV.

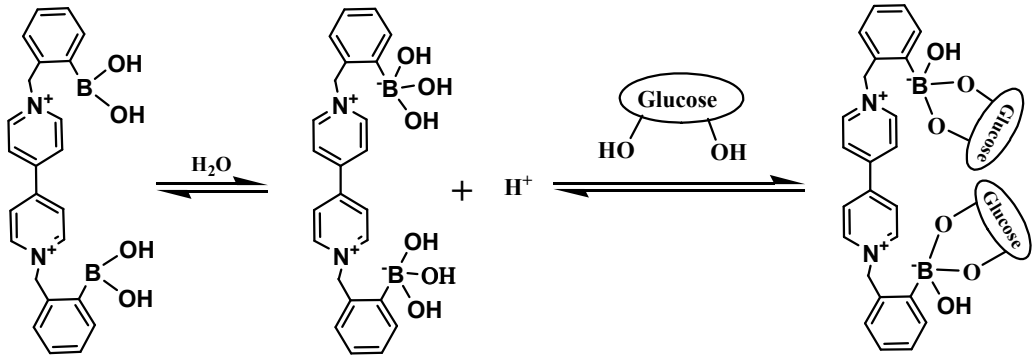

Fig. 5. Mechanism in the interaction between BBV and glucose.

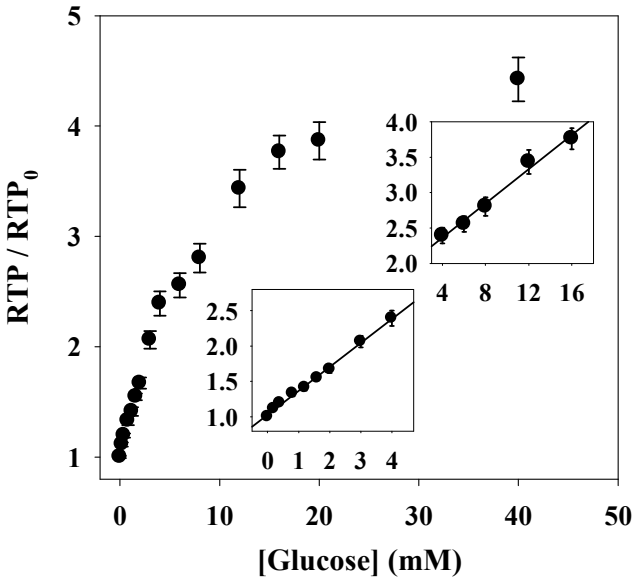

Fig. 6. Plots of RTP/RTP_0 as a function of glucose concentration show two linear ranges. Buffer, 10 mM PBS (pH 7.4); MPA-capped Mn-doped ZnS QDs, 40 mg L^{-1}; BBV, 1.6 μM.